European Journal of Medicinal Chemistry 44 (2009) 4937–4943

Contents lists available at ScienceDirect

European Journal of Medicinal Chemistry

journal homepage: http://www.elsevier.com/locate/ejmech

Original article

Effect of ruthenium complexation on trypanocidal activity of 5-nitrofuryl containing thiosemicarbazones

Mariana Pagano [a], Bruno Demoro [a], Jeanette Toloza [b], Lucía Boiani [c], Mercedes González [c], Hugo Cerecetto [c], Claudio Olea-Azar [b,**], Ester Norambuena [d], Dinorah Gambino [a,*], Lucía Otero [a,*]

[a] Cátedra de Química Inorgánica, Facultad de Química, Universidad de la República, Gral. Flores 2124, C.C. 1157, Montevideo 11800, Uruguay
[b] Departamento de Química Inorgánica y Analítica, Facultad de Ciencias Químicas y Farmacéuticas, Universidad de Chile, Santiago, Chile
[c] Laboratorio de Química Orgánica, Facultad de Química-Facultad de Ciencias, Universidad de la República, Iguá 4225, Montevideo 11400, Uruguay
[d] Departamento de Química, Facultad de Ciencias Básicas, Universidad Metropolitana de Ciencias de la Educación, Santiago, Chile

ARTICLE INFO

Article history:
Received 24 June 2009
Received in revised form
18 August 2009
Accepted 19 August 2009
Available online 29 August 2009

Keywords:
Chagas disease
Ruthenium complexes
5-Nitrofuryl containing thiosemicarbazones

ABSTRACT

In the search of new therapeutic tools for the treatment of American Trypanosomiasis, the largest parasitic disease burden in the American continent, three series of novel ruthenium complexes of the formula $[RuCl_2(HL)_2]$, $[RuCl_3(dmso)(HL)]$ and $[RuCl(PPh_3)(L)_2]$ with bioactive 5-nitrofuryl containing thiosemicarbazones as ligands (HL neutral, L monoanionic) were synthesized and characterized. Their *in vitro* growth inhibition activity against *Trypanosoma cruzi* and the effect of co-ligands in related physicochemical properties *i.e.* nitro moiety redox potential, lipophilicity and free radical scavenger capacity were evaluated. Results show that although a loss of activity was observed as a consequence of ruthenium complexation, lipophilicity and free radical scavenger capacity of the obtained complexes could be correlated to their trypanocidal effect.

1. Introduction

American trypanosomiasis or Chagas' disease, caused by the parasitic protozoa *Trypanosoma cruzi*, is a major public health concern in Latin America. In spite of the fact that the enforcement of public health programs, e.g. vector control, has decreased the incidence of new infections, it continues to be endemic in large areas of Central and South America and the sanitary problem associated with those already infected still remains a challenge. The drugs that have been commonly used to treat Chagas' disease were nifurtimox (Nfx, 4[(5-nitrofurfurylidene)amino]-3-methylthiomorpholine-1,1-dioxide), a nitrofuran derivative, and benznidazole (*N*-benzyl-2-nitroimidazole-1-acetamide), a nitroimidazole derivative. Both drugs show trypanocidal effect on all forms of the parasite but they can cause systemic toxicity and adverse effects. Therefore, the urgent need for more efficacious and safe chemotherapeutic approaches for the treatment of Chagas' disease is evident. [1–5].

On the other hand, the many activities of metal ions in biology have stimulated the development of metal-based chemotherapeutics in different fields of medicine. Although emphasis has been placed mainly on cancer treatment as a result of the great success of cisplatin, recent studies have also included parasitic diseases [6,7]. In this sense, the development of metal complexes with bioactive molecules as ligands has been used as a strategy to modify the ligand's pharmacological profile and/or obtain compounds that could act through a dual mechanism of action combining metal and ligand's toxic properties [7]. Anyway, biological properties of the metal-ligand species will depend not only on the nature of the ligand and the metal but also on the co-ligands and especially on the structural and physicochemical characteristics of the complex.

Based on this approach, our group has developed a series of different metal complexes with antichagasic ligands containing the 5-nitrofuryl pharmacophore. Such ligands, like Nfx, act on *T. cruzi* through free radical generation and redox cycling during their metabolism. The effect of rhenium, ruthenium, palladium and platinum complexation on the antiparasitic activity of selected semicarbazone or thiosemicarbazone ligands had been stated. Most complexes resulted more or at least equally active than the corresponding ligands and if not, the lack of activity of some of them could be related to properties like solubility, stability, lipophilicity or protein interaction. Moreover, it had been stated that the mechanism of action of the obtained complexes is the same than

* Corresponding author. Tel.: +59829249739; fax: +59829241906.
** Corresponding author. Tel.: +5626782834; fax: +5627370567.
E-mail addresses: colea@uchile.cl (C. Olea-Azar), dgambino@fq.edu.uy (D. Gambino), luotero@fq.edu.uy (L. Otero).

0223-5234/$ – see front matter © 2009 Elsevier Masson SAS. All rights reserved.
doi:10.1016/j.ejmech.2009.08.008

that of the ligands i.e. bioreduction and redox cycling. Additionally, in some cases a simultaneous new mechanism of action was evidenced [8–13].

In order to try to modulate the physicochemical properties of metal complexes potentially active against Chagas disease, a series of ruthenium complexes were rationally designed. Changes not only on the bioactive ligand but also on the oxidation state of the metal and the co-ligands were performed. In this sense, including different co-ligands that could influence complexes lipophilicity in the designed ruthenium complexes would let know the effect of this property on their biological activities. Selected bioactive ligands were 5-nitrofuryl containing thiosemicarbazones previously studied. Ruthenium was selected as central atom not only because of its pharmacological interest [14] but also for the availability of both +2 and +3 oxidation states from the synthetic precursors that can contribute with different co-ligands to the final mixed-ligand complexes [15–17].

In this work, the synthesis, characterization and anti *T. cruzi* activity of different ruthenium complexes with thiosemicarbazones (**HL1**–**HL4**) shown in Fig. 1 as active ligands are reported. Complexes' capability to produce free radicals as part of their mechanism of parasitic toxicity was studied by cyclic voltammetry and ESR techniques. In addition, in order to study the free radical scavenger properties of this family of compounds, oxygen radical absorbance capacity (using fluorescein (FL) as probe, $ORAC_{FL}$) studies were performed.

2. Results and discussion

2.1. Chemistry

Eleven different new ruthenium complexes with the 5-nitrofuryl containing thiosemicarbazones shown in Fig. 1 as ligands were synthesized and characterized. All obtained compounds are non conducting electrolytes and C, H, N and S analyses are in agreement with the proposed formula.

Four new ruthenium (II) complexes of the formula $[RuCl_2(HL)_2]$ with HL = **HL1** – **HL4** (in their neutral form, Scheme 1), were obtained in good yields and pure enough (purity determined by C, H, N and S analyses) to be used in the rest of the studies without further purification. Even if a Ru(III) complex ($Na[RuCl_4(dmso)_2]$) or a Ru(II) one ($[RuCl_2(dmso)_4]$) is used as a starting material, only the reported Ru(II) complexes, $[RuCl_2(HL)_2]$, were obtained for a 1:2 metal to ligand ratio. Similar results had been previously observed when obtaining ruthenium 5-nitrofuryl containing semicarbazone complexes [8]. On the other hand, when using a 1:1 metal to ligand molar ratio, Ru(III) complexes of the formula $[RuCl_3(dmso)(HL)]$ with HL = **HL1** – **HL4** were obtained in all studied experimental conditions. An excess of thiosemicarbazone ligand seems to create a reductive medium for the stabilization of +2 oxidation state for the metal. When using the five coordinate starting complex $[RuCl_2(PPh_3)_3]$, oxidation of the central atom occurred and three Ru(III) complexes of the formulae $[RuCl(PPh_3)(L)_2]$ with L = **L1**, **L3** and **L4** (Scheme 1) were isolated. In this case, thiosemicarbazone ligands coordinate in the monoanionic form.

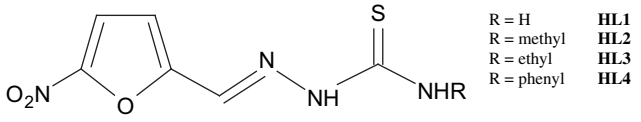

Fig. 1. 5-Nitrofuryl containing thiosemicarbazones.

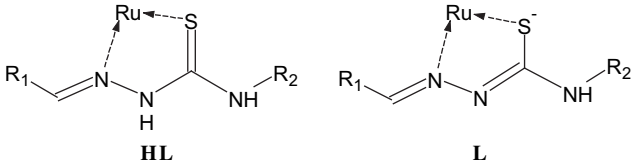

Scheme 1. Proposed modes of coordination of thiosemicarbazone ligands to ruthenium. R_1 = nitro furyl moiety, R_2 = H (**HL1**, **L1**), methyl (**HL2**, **L2**), ethyl (**HL3**, **L3**) or phenyl (**HL4**, **L4**).

2.2. IR studies

The IR vibrational spectroscopic behavior of all ruthenium complexes was studied in the solid state and compared with that previously reported for the free ligands and their palladium(II) and platinum(II) complexes [11,12,15]. Comparison of ruthenium complexes' IR spectra with those previously reported for palladium and platinum metal complexes allowed to determine the mode of coordination of these ligands in the obtained complexes. Complexes of the series $[RuCl_2(HL)_2]$ and $[RuCl_3(dmso)(HL)]$ showed an almost identical band shift pattern of the thiosemicarbazone ligands to that obtained for $[MCl_2(HL)]$ complexes (M = Pd or Pt). In the latter, thiosemicarbazone ligands coordinate to the metal as neutral ligands in a bidentate manner through thiocarbonyl sulfur and iminic nitrogen (**HL**, Scheme 1) [11,12]. Therefore, this mode of coordination can be assumed for the mentioned ruthenium complexes. On the other hand, a monoanionic and bidentate manner (L, Scheme 1) can be assumed for $[RuCl(PPh_3)(L)_2]$ complexes as the obtained shift pattern of the coordinated thiosemicarbazone ligands resulted very similar to that of $[ML_2]$ complexes (M = Pd or Pt) [11,12,15].

Moreover, the N, S mode of coordination obtained in all ruthenium complexes, is also evident through the assignment of ν(C=N), ν(C=S) and ν(N–N) bands whose shifts are diagnostic of this mode of coordination. Although, as it has been previously stated, bands assignments resulted difficult to perform for this kind of ligands, some of them are shown in Table 1 [11,12,15].

As shown in Table 1, after coordination clear changes in the wave number of the ν(C=N) bands of the free thiosemicarbazone ligands, at approximately 1500–1600 cm^{-1}, are observed. This modification is consistent with coordination of the thiosemicarbazone ligands

Table 1
Tentative assignment of the main characteristic IR bands of the ligands and their ruthenium complexes.

Compound	ν(C=N)	$\nu_s(NO_2)$	ν(N–N)	$\delta(NO_2)$ + Furan[a]	Other bands
HL1	1602	1356	1108	811	
$[RuCl_2(HL1)_2]$	1590	1351	1168	812	
$[RuCl_3(dmso)(HL1)]$	1590	1351	1168	811	ν(SO) 1089
$[RuCl(PPh_3)(L1)_2]$	1605	1349	1165	809	1430, 696, 525
HL2	1599	1354	1114	808	
$[RuCl_2(HL2)_2]$	1551	1350	1168	810	
$[RuCl_3(dmso)(HL2)]$	1556	1351	1166	811	
HL3	1602	1352	1104	805	
$[RuCl_2(HL3)_2]$	1597	1349	1154	809	
$[RuCl_3(dmso)(HL3)]$	1598	1350	1156	810	ν(SO) 1089
$[RuCl(PPh_3)(L3)_2]$	1570	1347	1156	807	1431, 697, 524
HL4	1595	1344	1104	811	
$[RuCl_2(HL4)_2]$	1598	1349	1185	811	
$[RuCl_3(dmso)(HL4)]$	1602	1350	1184	812	ν(SO) 1080
$[RuCl(PPh_3)(L4)_2]$	1597	1349	1198	808	1433, 694, 511

ν: stretching; δ: bending; s: strong, m: medium; w: weak.
[a] $\delta(NO_2)$ + furan modes or furan hydrogen wagging symmetric modes.

through the iminic nitrogen. On the other hand, the shift to higher wave numbers of the ν(N–N) band, observed in the obtained complexes, has also been related to the electronic delocalization produced as a consequence of coordination through the iminic nitrogen atom and/or deprotonation of the thiosemicarbazone ligands [11,12,15]. In addition, ν(C═S) bands at around 820–850 cm^{-1}, should shift to lower wave numbers when thiosemicarbazones act as N, S bidentate ligands but as it had been previously stated, they could not be unambiguously assigned for the complexes.

In agreement with the reported formulae of the complexes, the ν(NH) band, at approximately 3120–3150 cm^{-1}, is present in all $[RuCl_2(HL)_2]$ and $[RuCl_3(dmso)(HL)]$ complexes indicating that the ligand is non deprotonated in these neutral complexes. In contrast, ν(NH) band is not observed for the $[RuCl(PPh_3)(L)_2]$ complexes due to deprotonation of the ligands. In addition a band in c.a. 1100 cm^{-1} is present in all $[RuCl_3(dmso)(HL)]$ complexes showing the presence of sulfur coordinated dmso [8]. On the other hand, coordinated triphenylphosphine bands in c.a. 1400, 690 and 520 cm^{-1}, can be observed in $[RuCl(PPh_3)(L)_2]$ complexes spectra [15].

2.3. Cyclic voltammetry experiments

All ruthenium complexes displayed comparable voltammetric behaviour in DMSO but some differences were observed in relation to the previously reported palladium and platinum complexes [11,12]. For the ligands and all metal complexes, a well-defined wave (see Table 2 for ruthenium complexes' peak potentials) corresponding to a quasireversible process involving a one-electron transfer that had been assigned to the generation of the anion radical $RNO_2^{\bullet-}$ by reduction of the nitro group was observed. However, subsequent less negative cathodic waves that were observed for the free ligands and palladium and platinum complexes were not detected for the ruthenium ones in the potential range studied. The potentials of processes involved in these couples *i.e.* the reduction of nitro anion radical generated in the first couple and the reduction of the imine moiety (CH═N) of the thiosemicarbazone group, seems to be strongly affected as a consequence of ruthenium complexation.

Table 2
Reduction potentials of the nitro moiety for the obtained ruthenium complexes and the corresponding ligands measured in DMSO at 2000 mV/s. Potentials are reported in Volts vs. saturated calomel electrode.

Compound	E_{pc}[c]	E_{pa}[d]
HL1[a]	−0.84	−0.75
$[RuCl_2(HL1)_2]$	−0.98	−0.77
$[RuCl_3(dmso)(HL1)]$	−0.99	−0.74
$[RuCl(PPh_3)(L1)_2]$	−1.09	−0.72
HL2[a]	−0.79	−0.71
$[RuCl_2(HL2)_2]$	−1.02	−0.77
$[RuCl_3(dmso)(HL2)]$	−0.92	−0.73
HL3[a]	−0.79	−0.71
$[RuCl_2(HL3)_2]$	−1.12	−0.69
$[RuCl_3(dmso)(HL3)]$	−0.96	−0.69
$[RuCl(PPh_3)(L3)_2]$	−0.87	−0.73
HL4[a]	−0.78	−0.70
$[RuCl_2(HL4)_2]$	−0.94	−0.77
$[RuCl_3(dmso)(HL4)]$	−1.01	−0.72
$[RuCl(PPh_3)(L4)_2]$	−1.03	−0.72
Nfx[b]	−0.91	−0.85

[a] From Ref. [11].
[b] From Ref. [17].
[c] Cathodic peak potential.
[d] Anodic peak potential.

On the other hand, it should be stated that a self-protonation cathodic prepeak at around 0.4 V vs. SCE was observed only for $[RuCl_2(HL)_2]$ and $[RuCl_3(dmso)(HL)]$ complexes. This peak had also been observed for palladium and platinum complexes in which the thiosemicarbazone ligands were coordinated to the metal in a non deprotonated manner as it is proposed for $[RuCl_2(HL)_2]$ and $[RuCl_3(dmso)(HL)]$ complexes. Accordingly, $[RuCl(PPh_3)(L)_2]$ complexes did not show the prepeak because they do not have the capability to protonate the nitro group since the most acidic NH proton of the ligands was lost as a consequence of coordination to ruthenium.

The biological significance of the reduction potential of the nitro moiety present in the thiosemicarbazone active ligand in relation to the ability of the compounds to be bioreduced in the parasite leading to the toxic nitro anion radical species had been previously stated in Ref. [11]. Therefore, the effect of complex formation on this peak potential was studied. Table 2 shows the reduction potentials of the nitro moiety for the obtained ruthenium complexes and the corresponding ligands. Small changes were observed in the corresponding values as a consequence of complexes' formation and all of them are quite similar to the previously reported for the reference drug Nfx. However, all of them resulted higher than the observed for the corresponding ligands which could have a negative effect on the complexes biological activity as they would be more difficultly bioreduced.

2.4. ESR experiments

The free radicals generated in the electrochemical processes were characterized by ESR using "in situ" electrochemical reduction in DMSO, applying a potential corresponding to the first monoelectronic wave obtained from the cyclic voltammetric experiments.

The ESR spectra of the different radicals could be simulated by using the experimental constants of hyperfine coupling, changing different parameters to find the major coincidence between the simulated spectra and the experimental ones. For the successful use of the simulation programs, the introduction of starting hyperfine coupling values is needed. These values are fitted in order to obtain a satisfactory correspondence with the experimental spectra.

One hyperfine pattern was found for all obtained ruthenium complexes. Different substituents in the thiosemicarbazone chain of the coordinated ligands did not seem to affect the hyperfine pattern of the complexes. Additionally, no differences were observed between $[RuCl_2(HL)_2]$, $[RuCl_3(dmso)(HL)]$ or $[RuCl(PPH_3)(L)_2]$ ones. So, neither the mode of coordination of the thiosemicarbazone ligand nor the ruthenium oxidation state, seems to affect the hyperfine constants for the electrochemically obtained free radical species.

The ESR spectra of ruthenium complexes were simulated in terms of one triplet corresponding to the nitrogen nucleus belonging to the nitro group and one triplet corresponding to the nitrogen of the iminic (C═N) thiosemicarbazone group and four doublets due to non equivalent hydrogens. Other nuclei presented hyperfine constant smaller than the line width. The obtained calculated hyperfine constants are listed in Table 3. Obtained results were similar to those previously reported for palladium complexes [17].

2.5. In vitro anti T. cruzi activity

Obtained ruthenium compounds were tested *in vitro* against epimastigote form of the parasite. The percentages of growth inhibition related to Nfx (used as reference drug), $rPGI_{Nfx}$, for the complexes and the corresponding ligands [18] are listed in Table 4.

Table 3
Hyperfine splitting (gauss) for the free radical of the ruthenium complexes.

Compound	aN[a]	aN[a]	aH[b]	aH[b]	aH[b]	aH[b]
$[RuCl_2(HL1)_2]$	7.2	3.6	4.0	1.6	1.2	1.1
$[RuCl_3(dmso)(HL1)]$	7.5	3.4	4.0	1.5	1.2	1.1
$[RuCl(PPH_3)(L1)_2]$	7.0	3.5	3.9	1.5	1.2	1.0
$[RuCl_2(HL2)_2]$	7.3	4.0	4.2	1.7	1.1	1.0
$[RuCl_3(dmso)(HL2)]$	7.5	3.6	4.2	1.5	1.1	1.0
$[RuCl_2(HL3)_2]$	7.5	3.8	4.2	1.4	1.2	1.0
$[RuCl_3(dmso)(HL3)]$	7.2	3.2	3.9	1.2	1.0	0.8
$[RuCl(PPH_3)(L3)_2]$	7.5	3.9	4.2	1.5	1.2	1.0
$[RuCl_2(HL4)_2]$	7.1	3.6	4.4	1.1	1.3	1.0
$[RuCl_3(dmso)(HL4)]$	6.8	3.0	3.5	1.2	1.1	1.0
$[RuCl(PPH_3)(L4)_2]$	7.1	3.5	4.5	1.1	1.3	1.1

[a] Hyperfine coupling constants for nitrogen nucleous.
[b] Hyperfine coupling constants for hydrogen nucleous.

All tested ruthenium compounds resulted less active than Nfx in the assayed conditions. Moreover, ligands activity seems to diminish as a consequence of ruthenium complexation. Similar results had been reported for ruthenium complexes with bioactive 5-nitrofuryl containing semicarbazones as ligands [10]. Previously given explanations for these facts, like protein interaction could also be applied for these ruthenium thiosemicarbazone complexes. However, the very low solubility of all obtained ruthenium complexes in water could also be the reason for the observed lack of anti *T. cruzi* activity as they might partially precipitate from the aqueous culture medium. This fact could cause that the dose that reaches the parasite to be smaller than supposed provoking a lower effect on the parasite growing On the other hand, as it has been previously stated, reduction potential of the nitro moiety for all the obtained complexes resulted higher than the observed for the corresponding ligands. This fact could also explain the decrease in complexes biological activity respect to the ligands as the former would be more difficultly bioreduced *in vivo*.

No differences in the observed biological activity of $[RuCl_2(HL)_2]$ and $[RuCl_3(dmso)(HL)]$ complexes were observed. However, as the latter have only one mole of bioactive ligand per mole of complex, it should be stated that their activity per mol of thiosemicarbazone ligand is higher than for the former. For each ligand, $[RuCl(PPh_3)(L)_2]$ complexes resulted as the most active ones.

Table 4
In vitro biological activity and R_M values of ruthenium complexes and the corresponding ligands.

Compound	$rPGI_{Nfx}$[a]	$R_{M(60:40)}$[c]	$R_{M(90:10)}$[d]
HL1	1.5[b]	−1.19	
$[RuCl_2(HL1)_2]$	0.5	−0.50	
$[RuCl_3(dmso)(HL1)]$	0.4	−0.50	
$[RuCl(PPh_3)(L1)_2]$	0.8		−0.95
HL2	1.1[b]	−0.47	
$[RuCl_2(HL2)_2]$	0.3	0.27	
$[RuCl_3(dmso)(HL2)]$	0.3	0.27	
HL3	1.1[b]	−0.29	
$[RuCl_2(HL3)_2]$	0.3	0.52	
$[RuCl_3(dmso)(HL3)]$	nd	0.52	
$[RuCl(PPh_3)(L3)_2]$	0.6		−0.18
HL4	0.3[b]	0.18	−0.95
$[RuCl_2(HL4)_2]$	nd	0.95	−0.60
$[RuCl_3(dmso)(HL4)]$	0.3	0.95	
$[RuCl(PPh_3)(L4)_2]$	0.4		0

[a] $rPGI_{Nfx}$: Ratio of percentage of growth inhibition of *T. cruzi* epimastigote cells at 5 μM (for the ligands) or 25 μM (for the complexes) with respect to Nfx (PGI of Nfx was taken as 1.0).
[b] From Ref. [11]; nd: not determined.
[c] Elution mixture dmso/physiological serum 60:40, v/v.
[d] Elution mixture dmso/physiological serum 90:10, v/v.

2.6. Lipophilicity studies

Lipophilicity was experimentally determined in order to study the effect of coordination to ruthenium on thiosemicarbazone ligands' physicochemical properties. Additionally, the effect of different co-ligands present in the complexes on their lipophilicity was determined trying to obtain a correlation with the anti *T. cruzi* activity. Reversed-phase TLC experiments were performed for all the derivatives on precoated TLC-C18 and eluted with different mixtures of dmso/physiological serum (60:40 or 90:10, v/v). It was not possible to use a unique elution mixture for separating all assayed compounds as lipophilicities were too different. If the elution was performed using the 60:40 dmso/physiological serum mixture, ligands could be separated from both $[RuCl_2(HL)_2]$ and $[RuCl_3(dmso)(HL)]$ complexes but all $[RuCl(PPh_3)(L)_2]$ complexes, as lipophilic entities, remained in the origin of the chromatographic plate. For the 90:10 mixture all complexes and ligands, except the less polar **HL4**, $[RuCl_2(HL4)_2]$ and all $[RuCl(PPh_3)(L)_2]$ complexes, run with the front of the elution mixture. The R_f values were converted into R_M values via the relationship: $R_M = \log[(1/R_f) - 1]$. Table 4 summarizes R_M for each compound in each elution condition.

As expected, ligands' lipophilicity increases as the non polar N_4 substituent changes from H to phenyl (Fig. 1). $[RuCl_2(HL)_2]$ and $[RuCl_3(dmso)(HL)]$ complexes resulted more lipophilic than the corresponding ligands. The presence of dmso in the coordination sphere does not seem to affect complexes' lipophilicity as no differences in R_M values between $[RuCl_2(HL)_2]$ and $[RuCl_3(dmso)(HL)]$ complexes were observed in the assayed conditions. Comparing **HL4** and its $[RuCl(PPh_3)(L4)_2]$ complex, an increase in lipophilicity is also observed and the latter resulted more lipophilic than $[RuCl_2(HL4)_2]$. A similar behavior could be expected for all the ligands and their corresponding $[RuCl(PPh_3)(L)_2]$ complexes being $[RuCl(PPh_3)(L)_2]$ complexes the most lipophilic compounds. The presence of a bulky non polar co-ligand, triphenylphosphine, in these complexes' coordination sphere would be responsible for the observed results. Additionally, the same tendency observed for the ligands' lipophilicity is conserved in all ruthenium complexes, being all **HL4** complexes the most lipophilic of each series of ruthenium compounds.

Lipophilicity could be correlated to the *in vitro* anti-*T. cruzi* activity. Although, a statistically acceptable correlation between both parameters involving all the population was not obtained, some tendency in the series could be evidenced (Fig. 2). When only the complexes were analyzed lipophilicity seems to play a relevant role in the activity (compare activities and lipophilicity changes between $[RuCl(PPh_3)(L1)_2]$ and $[RuCl_2(HL1)_2]$ or $[RuCl(PPh_3)(L3)_2]$ and $[RuCl_2(HL3)_2]$). For each case, $[RuCl(PPh_3)(L)_2]$ complexes that resulted the most active, are also the most lipophilic. However, although ruthenium complexation increases lipophilicity respect to the ligands, it does not increase the biological activity. On the other hand, in the ligands' series, the opposite tendency is observed, i.e. **HL1**, the most hydrophilic thiosemicarbazone is the most active one (Fig. 2). As expected, lipophilicity is only one of the factors that could influence compounds biological activity. In this sense, the effect of the activity of the thiosemicarbazone ligand is evident being $[RuCl(PPh_3)(L1)_2]$ the most active complex as **HL1** is the most active ligand.

2.7. Free-radical scavenger capacity: $ORAC_{FL}$ assay

The antioxidant activities of the obtained ruthenium complexes were evaluated using the ORAC assay with ROO• species. As an example Fig. 3 shows the obtained curves for $[RuCl_2(HL1)_2]$. Trolox equivalent values, including correlation coefficients are given in Table 5. Results indicate that the free radical scavenger properties of

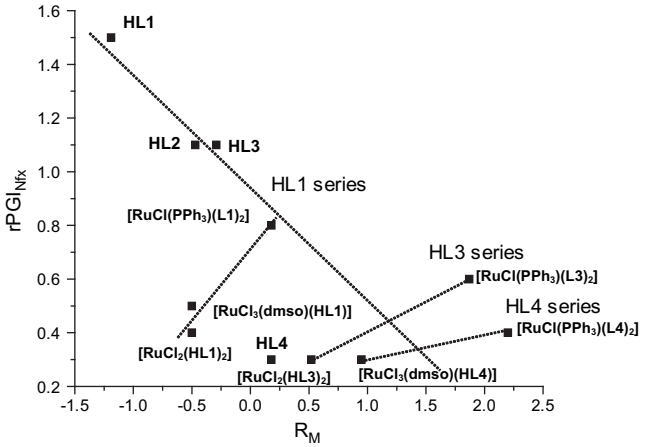

Fig. 2. $rPGI_{Nfx}$ vs. $R_{M,60:40}$ (dmso/physiological serum 60:40, v/v) for ligands and complexes. Notes: dotted-line shows the tendency; **HL2** series was omitted for simplicity; $R_{M,60:40}$ for $[RuCl(PPh_3)(L)_2]$ series were estimated from the corresponding $R_{M,90:40}$ (dmso/physiological serum 90:10, v/v) values.

Table 5
Trolox equivalents of the studied ruthenium complexes.

Compound	Trolox equivalents[a]	r^2
$[RuCl_2(HL1)_2]$	4.12	0.9848
$[RuCl_3(dmso)(HL1)]$	2.48	0.9825
$[RuCl(PPh_3)(L1)_2]$	2.65	0.9711
$[RuCl_2(HL2)_2]$	3.46	0.9913
$[RuCl_3(dmso)(HL2)]$	2.17	0.9509
$[RuCl_2(HL3)_2]$	4.01	0.9993
$[RuCl_3(dmso)(HL3)]$	2.10	0.9997
$[RuCl(PPh_3)(L3)_2]$	1.61	0.9823
$[RuCl_2(HL4)_2]$	2.35	0.9914
$[RuCl_3(dmso)(HL4)]$	2.28	0.9927
$[RuCl(PPh_3)(L4)_2]$	2.05	0.9931

[a] Expressed as μmol of Trolox equivalent/μmol of compounds.

the obtained compounds are low but they resulted higher than those previously reported for the free thiosemicarbazone ligands [19]. Coordination to ruthenium seems to increase the acidity of the ligands' protons, probably increasing their antioxidant activity. For each ligand, complexes of the formula $[RuCl_2(HL)_2]$ had the highest Trolox equivalent values as they have two coordinated thiosemicarbazone ligands. However, $[RuCl(PPh_3)(L)_2]$ complexes, also presenting two coordinated thiosemicarbazone ligands, resulted the less active as the corresponding ligands are deprotonated in these complexes.

On the other hand, taking into account that trypanocidal activity of the ruthenium compounds is supposed to involve toxic free radical species generated *in vivo*, the free radical scavenger capacity of the complexes could be considered as a protective effect for the parasites and consequently, as negative fact for complexes druggability. In these sense, it should be noted that complexes of the formula $[RuCl(PPh_3)(L)_2]$ having the lowest antioxidant activity, are the most toxic for the parasites. These compounds would not scavenge their own produced free radicals what could increase the toxic effect on the parasite.

3. Conclusions

Three series of mixed-ligand ruthenium complexes of the formula $[RuCl_2(HL)_2]$, $[RuCl_3(dmso)(HL)]$ and $[RuCl(PPh_3)(L)_2]$ with bioactive 5-nitrofuryl containing thiosemicarbazones were synthesized and characterized. Although, coordination to ruthenium seems to decrease the ligands' anti *T. cruzi* activity, the effect of the presence of different co-ligands on the activity and related physicochemical properties resulted evident. In the light of this, while a high lipophilicity seems to favor the trypanocidal effect, the free radical scavenger capacity of the obtained complexes could be correlated to a lower biological activity.

4. Experimental protocols

4.1. Materials and general procedures

All common laboratory chemicals were purchased from commercial sources and used without further purification. $[RuCl_2(dmso)_4]$, $Na[RuCl_4(dmso)_2]$ and $[RuCl_2(PPh_3)_3]$, with dmso = dimethylsulfoxide and PPh_3 = triphenylphosphine, were prepared according to literature procedures [20–22]. All thiosemicarbazone ligands (*E* form) were synthesized using the previously reported methodology [18]. C, H, N and S analyses were performed with a Carlo Erba Model EA1108 elemental analyzer. Conductimetric measurements were performed at 25 °C in 10^{-3} M dimethylformamide (DMF) solutions using a Conductivity Meter 4310 Jenway. FTIR spectra (4000–400 cm^{-1}) of the complexes and the free ligands were measured as KBr pellets with a Bomen FTIR model M102 instrument. Electronic spectra were recorded on a Spectronic 3000 spectrophotometer.

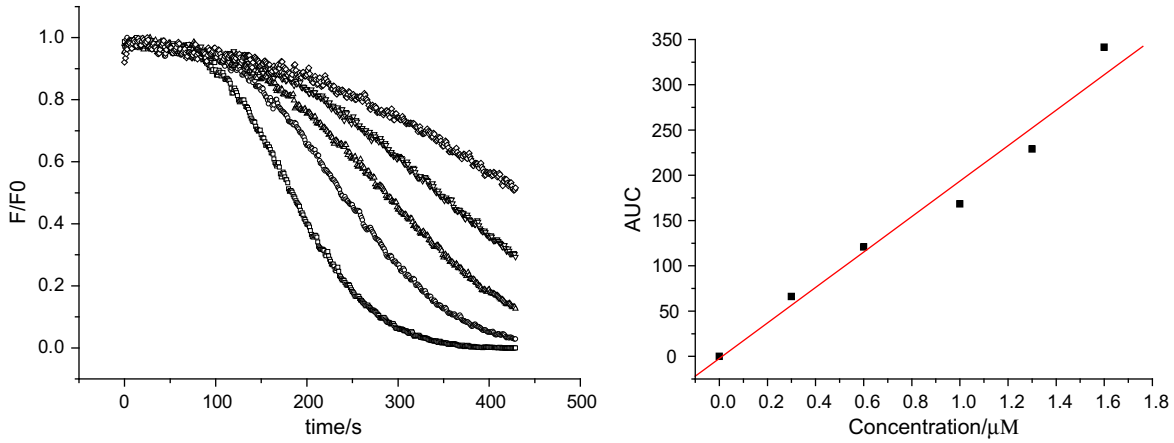

Fig. 3. Effect of the addition of different concentrations of $[RuCl_2(HL1)_2]$ on fluorescence curve and the corresponding AUC curve.

4.2. Synthesis

4.2.1. General procedure for $[RuCl_2(HL)_2]$ complexes

$[RuCl_2(dmso)_4]$ (50 mg, 0.10 mmol) and the corresponding ligand (0.24 or 0.20 mmol) were heated under reflux in ethanol (10 mL) for **HL1** and **HL2** or ethanol–isopropanol (7:3) (10 mL) for **HL3** and **HL4** during 24 h, after which a dark brown microcrystalline solid precipitated. The solid was filtered off and washed with hot ethanol. The same results are observed using $Na[RuCl_4(dmso)_2]$ as starting material.

4.2.1.1. $[RuCl_2(HL1)_2]$. Yield: 40% (30 mg) $\lambda_{max.}$ (ethanol): 400 nm% Anal.(Calc.) for $C_{12}H_8N_8O_6S_2Cl_2Ru$: C 23.81 (24.01), N 18.36 (18.66), H 2.11 (2.01), S 10.70 (10.71).

4.2.1.2. $[RuCl_2(HL2)_2]$. Yield: 50% (38 mg). $\lambda_{max.}$ (ethanol): 402 nm% Anal.(Calc.) for $C_{14}H_{12}N_8O_6S_2Cl_2Ru$: C 26.31 (26.76), N 17.80 (17.83), H 2.23 (2.57), S 10.38 (10.20).

4.2.1.3. $[RuCl_2(HL3)_2]$. Yield: 40% (30 mg). $\lambda_{max.}$ (ethanol): 403 nm% Anal.(Calc.) for $C_{16}H_{16}N_8O_6S_2Cl_2Ru$: C 29.45 (29.27), N 16.80 (17.07), H 2.91 (3.07), S 9.50 (9.77).

4.2.1.4. $[RuCl_2(HL4)_2]$. Yield: 55% (50 mg). $\lambda_{max.}$ (ethanol): 412 nm% Anal.(Calc.) for $C_{24}H_{16}N_8O_6S_2Cl_2Ru$: C 38.29 (38.30), N 14. 90 (14.89), H 2.44 (2.68), S 8.23 (8.52).

4.2.2. General procedure for $[RuCl_3(dmso)(HL)]$ complexes

$Na[RuCl_4(dmso)_2]$ (50 mg, 0.12 mmol) or $[RuCl_2(dmso)_4]$ (50 mg, 0.10 mmol) and the corresponding ligand (0.10 mmol) were heated under reflux in isopropanol (10 mL) for **HL1** and **HL2** or ethanol–isopropanol (7:3) (10 mL) for **HL3** and **HL4** during 24 h, after which a brown microcrystalline solid precipitated. The solid was filtered off and washed with ethanol.

4.2.2.1. $[RuCl_3(dmso)(HL1)]$. Yield: 54% (30 mg). $\lambda_{max.}$ (ethanol): 402 nm% Anal.(Calc.) for $C_{14}H_{16}N_8O_7S_3Cl_3Ru$: C 19.45 (19.23), N 11.39 (11.21), H 2.10 (2.42), S 12.40 (12.63).

4.2.2.2. $[RuCl_3(dmso)(HL2)]$. Yield: 45% (23 mg). $\lambda_{max.}$ (ethanol): 404 nm% Anal.(Calc.) for $C_{16}H_{20}N_8O_7S_3Cl_3Ru$: C 21.21 (21.04), N 10.71 (10.90), H 3.03 (2.75), S 12.15 (12.48).

4.2.2.3. $[RuCl_3(dmso)(HL3)]$. Yield: 40% (20 mg). $\lambda_{max.}$ (ethanol): 407 nm% Anal.(Calc.) for $C_{18}H_{24}N_8O_7S_3Cl_3Ru$: C 22.70 (22.76), N 10.26 (10.61), H 2.99 (3.06), S 11.90 (12.15).

4.2.2.4. $[RuCl_3(dmso)(HL4)]$. Yield: 30% (17 mg). $\lambda_{max.}$ (ethanol): 416 nm% Anal.(Calc.) for $C_{26}H_{24}N_8O_7S_3Cl_3Ru$: 29.41 (29.20), 9.88 (9.73), 3.04 (2.80), 11.13 (11.14).

4.2.3. General procedure for $[RuCl(PPh_3)(L)_2]$ complexes

$[RuCl_2(PPh_3)_3]$ (50 mg, 0.05 mmol) and the corresponding ligand (0.10 mmol) were heated under reflux in ethanol for 8 h, after which a violet microcrystalline solid precipitated. The solid was filtered off and thoroughly washed with hot ethanol.

4.2.3.1. $[RuCl(PPh_3)(L1)_2]$. Yield: 23% (9 mg). $\lambda_{max.}$ (acetone): 416, 548 nm% Anal.(Calc.) for $C_{30}H_{25}N_8O_6S_2PClRu$: C 44.05 (43.67), N 13.70 (13.58), H 3.10 (3.05), S 7.72 (7.77).

4.2.3.2. $[RuCl(PPh_3)(L3)_2]$. Yield: 20% (8 mg). $\lambda_{max.}$ (acetone): 420, 548 nm% Anal.(Calc.) for $C_{34}H_{33}N_8O_6S_2PClRu$: C 46.70 (46.34), N 12.71 (12.71), H 3.81 (3.77), S 6.95 (7.28).

4.2.3.3. $[RuCl(PPh_3)(L4)_2]$. Yield: 15% (7 mg). $\lambda_{max.}$ (acetone): 427, 550 nm% Anal.(Calc.) for $C_{42}H_{33}N_8O_6S_2PClRu$: C 51.74 (51.61), N 11.73 (11.46), H 3.39 (3.40), S 6.29 (6.56).

4.3. Cyclic voltammetry experiments

DMSO (spectroscopy grade) was obtained from Aldrich. Tetrabutylammonium perchlorate (TBAP), used as supporting electrolyte, was obtained from Fluka. Cyclic voltammetry was carried out using a Metrohm 693 VA instrument with a 694 VA Stand convertor and a 693 VA Processor, in DMSO (ca. 1.0×10^{-3} M), under nitrogen atmosphere at room temperature, with TBAP (ca. 0.1 M), using a three-electrode cell. A mercury-dropping electrode was used as the working electrode, a platinum wire as the auxiliary electrode, and saturated calomel as the reference electrode.

4.4. ESR

Isotropic ESR spectra were recorded in X band (9.85 GHz) using a Bruker ECS 106 spectrometer with a rectangular cavity and 50 KHz field modulation. DPPH (α,α'-diphenyl-β-picrylhydrazyl radical) was employed as reference for spectrum calibration. The radical anions were generated by electrolytic reduction "in situ" at room temperature. Other conditions of measurements were as follows: power: 20.1 mW, attenuation: 10.0 dB, modulation amplitude: 0.49 gauss, receiver gain: 1×10^5, conversion time: 40.96 ms, time constant: 81 ms. Each spectrum was recorded with 15 scans. The hyperfine splitting constants were estimated to be accurate within 0.05 G. Simulation of the ESR spectra was achieved using the software WINEPR Simphonia 2.11 version.

4.5. Lipophilicity studies

Reversed-phase TLC experiments were performed on precoated TLC plates SIL RP-18W/UV_{254} and eluted with DMSO/physiological serum (60:40 or 90:10, v/v). Stock solutions were prepared in pure DMSO (Aldrich) prior to use. The plates were developed in a closed chromatographic tank, dried and the spots were located under UV light. The R_f values were averaged from three determinations, and converted into R_M values via the relationship: $R_M = \log [(1/R_f) - 1]$ [23].

4.6. *Trypanocidal* in vitro *test*

T. cruzi epimastigotes (Tulahuen 2 strain) were grown at 28 °C in an axenic medium (BHI-Tryptose) as previously described in Ref. [23,24] complemented with 5% fetal bovine serum. Cells from a 10-days old culture (stationary phase) were inoculated into 50 mL of fresh culture medium to give an initial concentration of 1×10^6 cells/mL. Before inoculation, the media was added to the indicated amount of the drug from a stock solution in DMSO. The final concentration of DMSO in the culture media never exceeded 0.4% and the control was run in the presence of 0.4% DMSO and in the absence of any drug. No effect on epimastigotes growth was observed by the presence of up to 1% DMSO in the culture media. The percentage of growth inhibition was calculated as follows: $PGI\ (\%) = \{1-[(np_p - np_{0p})/(np_c - np_{0c})]\} \times 100$, where np_p = is the number of parasite/mL of the culture medium incubated with the drug at day 5; np_{0p} = is the number of parasite/mL of the culture medium containing the drug just after addition of the inocula (day 0); np_c = is the number of parasite/mL of the culture medium in the absence of any drug (control) at day 5; np_{0c} = is the number of parasite/mL of the culture medium in the absence of the drug at day 0.

4.7. Free-radical scavenger capacity: $ORAC_{FL}$ assay

A luminescence spectrometer LS 50B (Perkin Elmer, Boston, MA, USA), a heating circulator bath DC1–B3 (Haake Fisons, Karlsruhe, Germany) and quartz cuvettes were used. For the $ORAC_{FL}$ assay, the 490-P excitation and 515-P emission filters were used, and the fluorescence measurement was carried out at 60 °C. The ORAC method of Ou et al. [25] was modified as follows: the reaction was carried out in 75 mM phosphate buffer (pH 7.4), and the final reaction volume was 3000 μL. A mixture of the studied compounds (15, 30, 45, 60 μL; 0.5–2.0 μM final concentrations) and fluorescein (FL) (215 μL; 70 nM final concentration) solutions was preincubated in the cuvette for 30 s at 60 °C. After the rapid addition of 2,2′-azobis(2-methylpropionamidine) dihydrochloride (AAPH) solution (240 μL; 12 mM final concentration) the fluorescence was recorded every minute for 12 min. As a blank FL and AAPH in phosphate buffer instead of the studied compounds solutions were employed and eight calibration solutions using 6-hydroxy-2,5,7,8-tetramethylchroman-2-carboxylic acid (Trolox) (1–8 μM, final concentration) as antioxidant positive control were also carried out in each assay. All the reaction mixtures were prepared in duplicate, and at least three independent assays were performed for each sample. Blank and antioxidant curves (fluorescence versus time) were first normalized by dividing original data by fluorescence at $t = 0$ s. From the normalized curves, the area under the fluorescence decay curve (AUC) was calculated as

$$\mathrm{AUC} = 1 + \sum_{i=1}^{i=12} \frac{f_i}{f_0}$$

where f_0 is the initial fluorescence reading at 0 min and f_i is the fluorescence reading at time *i*. The net AUC corresponding to each sample was calculated by subtracting the AUC corresponding to the blank. Regression equations between net AUC and antioxidant concentration were calculated for all the samples. $ORAC_{FL}$ values were expressed as Trolox equivalents by using the standard curve calculated for each assay. Final results were expressed in μmol of Trolox equivalent/μmol of samples [26].

Acknowledgements

This work was partially supported by TWAS Research Grant 02-036 RG/CHE/LA, ANII FCE 2007_188, Uruguay and FONDECYT 1071068 and 7070282, Chile. DG, HC and MG wish to thank RID-IMEDCHAG-CYTED.

References

[1] World Health Organization: http://www.who.int/ctd/chagas/burdens/.
[2] M. Paulino, F. Iribarne, M. Dubin, S. Aguilera-Morales, O. Tapia, A.O.M. Stoppani, The chemotherapy of Chagas disease: an overview. Mini-Rev. Med. Chem. 5 (2005) 499–519.
[3] J.D. Maya, B. Cassels, P. Iturriaga-Vásquez, J. Ferreira, M. Faúndez, N. Galanti, A. Ferreira, A. Morello, Mode of action of natural and synthetic drugs against *Trypanosoma cruzi* and their interaction with the mammalian host. Comp. Biochem. Physiol. A 146 (4) (2007) 601–620.
[4] H. Cerecetto, M. González, Chemotherapy of Chagas disease: status and new developments. Curr. Top. Med. Chem. 2 (2002) 1185–1190.
[5] C. Schofield, J. Jannin, R. Salvatella, The future of Chagas disease control. Trends Parasitol. 22 (2006) 583–588.
[6] R.A. Sánchez-Delgado, A. Anzellotti, Metal complexes as chemotherapeutic agents against tropical diseases: trypanosomiasis, malaria and leishmaniasis. Mini-Rev. Med. Chem. 4 (2004) 23–30.
[7] S.P. Fricker, R.M. Mosi, B.R. Cameron, I. Baird, Y. Zhu, V. Anastassov, J. Cox, P.S. Doyle, E. Hansell, G. Lau, J. Langille, M. Olsen, L. Qin, R. Skerlj, R.S.Y. Wong, Z. Santucci, J.H. McKerrow, Metal compounds for the treatment of parasitic diseases. J. Inorg. Biochem. 102 (2008) 1839–1845.
[8] L. Otero, P. Noblía, D. Gambino, H. Cerecetto, M. González, J.A. Ellena, O.E. Piro, Synthesis and characterization of new ruthenium complexes with active ligands against Chagas' disease. Inorg. Chim. Acta 344 (2003) 85–94.
[9] L. Otero, P. Noblía, D. Gambino, H. Cerecetto, M. González, R. Sánchez-Delgado, E. Castellano, O.E. Piro, New Re(V) nitrofuryl semicarbazone complexes. Crystal structure of $ReOCl_2(PPh_3)$(3-(5-Nitrofuryl)acroleine semicarbazone). Z. Anorg. Allg. Chem. 629 (2003) 1033–1036.
[10] L. Otero, G. Aguirre, L. Boiani, M. González, A. Denicola, C. Rigol, C. Olea-Azar, J.D. Maya, A. Morello, D. Gambino, H. Cerecetto, Nitrofurylsemicarbazone rhenium and ruthenium complexes as anti-trypanosomal agents. Eur. J. Med. Chem. 41 (2006) 1231–1239.
[11] L. Otero, M. Vieites, L. Boiani, A. Denicola, C. Rigol, L. Opazo, C. Olea-Azar, J.D. Maya, A. Morello, R.L. Krauth-Siegel, O.E. Piro, E. Castellano, M. González, D. Gambino, H. Cerecetto, Novel antitrypanosomal agents based on palladium nitrofurylthiosemicarbazone complexes: DNA and redox metabolism as potential therapeutic targets. J. Med. Chem. 49 (2006) 3322–3331.
[12] M. Vieites, L. Otero, D. Santos, D. Gajardo, J. Toloza, R. Figueroa, E. Norambuena, C. Olea-Azar, G. Aguirre, H. Cerecetto, M. González, A. Morello, J.D. Maya, B. Garat, D. Gambino, Platinum (II) metal complexes as potential anti-*Trypanosoma cruzi* agents. J. Inorg. Biochem 102 (2008) 1033–1043.
[13] M. Vieites, L. Otero, D. Santos, C. Olea-Azar, E. Norambuena, G. Aguirre, H. Cerecetto, M. González, U. Kemmerling, A. Morello, J.D. Maya, D. Gambino, Platinum-based complexes of bioactive 3-(5-nitrofuryl)acroleine thiosemicarbazones showing anti-*Trypanosoma cruzi* activity. J. Inorg. Biochem 103 (2009) 411–418.
[14] C.S. Allardyce, A. Dorcier, C. Scolaro, P.J. Dyson, Development of organometallic (organo-transition metal) pharmaceuticals. Appl. Organometal. Chem. 19 (2005) 1–10.
[15] D. Gambino, L. Otero, M. Vieites, M. Boiani, M. González, E.J. Baran, H. Cerecetto, Vibrational spectra of palladium 5-nitrofuryl thiosemicarbazone complexes: experimental and theoretical study. Spectrochim. Acta Part A Mol. Biomol. Spectrosc. 68 (2007) 341–348.
[16] C. Olea-Azar, A.M. Atria, F. Mendizábal, R. Di Maio, G. Seoane, H. Cerecetto, Electrón spin resonance and cyclic voltammetry studies of nitrofurane and nitrothiophene analogues of nifurtimox. Spectrosc. Lett. 31 (1998) 99–109.
[17] L. Otero, C. Folch, G. Barriga, C. Rigol, L. Opazo, M. Vieites, D. Gambino, H. Cerecetto, E. Norambuena, C. Olea-Azar, ESR, electrochemical and reactivity studies of antitrypanosomal palladium thiosemicarbazone complexes. Spectrochim. Acta Part A Mol. Biomol. Spectrosc. 70 (2008) 519–523.
[18] G. Aguirre, L. Boiani, H. Cerecetto, M. Fernández, M. González, A. Denicola, L. Otero, D. Gambino, C. Rigol, C. Olea-Azar, M. Faundez, In vitro activity and mechanism of action against the protozoan parasite *Trypanosoma cruzi* of 5-nitrofuryl containing thiosemicarbazones. Bioorg. Med. Chem. 12 (2004) 4885–4893.
[19] L. Otero, J.D. Maya, A. Morello, C. Rigol, G. Barriga, J. Rodriguez, C. Folch, E. Norambuena, M. Gonzalez, C. Olea-Azar, H. Cerecetto, D. Gambino, Insight into the bioreductive mode of action of antitrypanosomal 5-nitrofuryl containing thiosemicarbazones. Med. Chem. 4 (2008) 11–17.
[20] J.A. Stephenson, G. Wilkinson, New complexes of ruthenium(II) and (III) with triphenylfosfine, triphenylarsine, trichlorostannate, pyridine and other ligands. J. Inorg. Nucl. Chem. 28 (1966) 945–956.
[21] I. Evans, A. Spencer, G.J. Wilkinson, Dichlorotetrakis(dimethylsulfoxide)-ruthenium(II) and its use as a source material for some new ruthenium(II) complexes. Chem. Soc. Dalton Trans. (1973) 204–209.
[22] E. Alessio, G. Balducci, A. Lutman, G. Mestroni, M. Calligaris, W.M. Attia, Synthesis and characterization of two new classes of ruthenium(III) sulfoxide complexes with nitrogen donor ligands (L): Na[*trans*-$RuCl_4(R_2SO)$(L) and *mer*, *cis*-$RuCl_3(R_2SO)(R_2S\ O)$(L). The crystal structure of Na[*trans*-$RuCl_4$(DM *SO*)(NH_3)]·2DMSO, Na[*trans*-$RuCl_4$(DM *SO*)(Im)]·H2O, Me2CO and *mer*, *cis*-$RuCl_3$(DM *SO*)(DMS *O*)(NH_3). Inorg. Chim. Acta 203 (1993) 205–217.
[23] H. Cerecetto, R. Di Maio, M. González, M. Risso, P. Saenz, G. Seoane, A. Denicola, G. Peluffo, C. Quijano, C. Olea-Azar, 1,2,5-Oxadiazole *N*-oxide derivatives and related compounds as potential antitrypanosomal drugs. Structure–activity relationships. J. Med. Chem. 42 (1999) 1941–1950.
[24] L. Huang, A. Lee, J.A. Ellman, Identification of potent and selective mechanism-based inhibitors of the cysteine protease cruzain using solid-phase parallel synthesis. J. Med. Chem. 45 (2002) 676–684.
[25] B. Ou, M. Hampsch-Woodill, R.L. Prior, Development and validation of an improved oxygen radical absorbance capacity assay using fluorescein as the fluorescent probe. J. Agric. Food Chem. 49 (2001) 4619–4626.
[26] A. Dávalos, C. Gómez-Cordovés, B. Bartolomé, Extending applicability of the oxygen radical absorbance capacity (ORAC − Fluorescein) assay. J. Agric. Food Chem. 52 (2004) 48–54.